ChemComm

COMMUNICATION

View Article Online
View Journal | View Issue

Cite this: *Chem. Commun.*, 2024, **60**, 14037

Received 15th October 2024,
Accepted 30th October 2024

DOI: 10.1039/d4cc05463f

rsc.li/chemcomm

Synthesis of heteroleptic bis-phosphine bis-NHC iron (0) complexes: a strategy to enhance small molecule activation†

Christian M. Andre and Nathaniel K. Szymczak *

We report the synthesis of heteroleptic iron complexes supported by both a bis-phosphine ligand (depe) and a bis-NHC ligand. The mixed ligand sets provide access to iron (0) adducts of N_2 and CO that are highly activated, in comparison to homoleptic (*i.e.* Fe(depe)$_2$L) variants. Computational and experimental studies revealed the mixed ligand set distorts the geometric and electronic structure to yield an unusually basic iron. Although protonation occurred at Fe, silylation of the Fe(0)N_2 complex afforded a highly activated silyldiazenido [FeNNSiMe$_3$]$^+$ complex.

Low-valent iron complexes are routinely targeted as models for Fe-nitrogenase, given their ability to activate N_2‡ as well as other small molecules (CO, CO_2, *etc.*),[1] with iron phosphines among the most established (Fig. 1A).[2] Of particular note is the Fe^0N_2 complex of 1,2-bis(diethylphosphino)ethane (depe) because it features a significantly activated N_2 ligand and is a catalyst for selective N_2 reduction to hydrazine.[2a] These properties have motivated studies by our group[3] and others[4] to examine additional design principles, such as those achieved by introducing secondary sphere acids, to further enhance the activation imparted by the Fe^0(depe)$_2$ unit to small molecules. While adjusting the primary coordination sphere of the iron centre to increase its electron density is the most common redesign strategy, modification of the phosphine from depe typically§ affords systems that are less donating than Fe(depe)$_2$[5] and/or have a dramatically different steric profile and binding geometry.[2i,j,6] In analogy to phosphines, lower-coordinate iron complexes of monodentate N-heterocyclic carbenes (NHC) are reported to activate N_2 to a greater extent (Fig. 1B), a result of their stronger σ-donor ability than phosphines.[7]

In contrast to the breadth of low-valent chemistry reported with phosphine donors, there are no such examples of 18-electron Fe^0 complexes containing four NHC donors.[8] To bridge the gap between Fe^0 complexes containing four phosphines (known) and those containing four NHCs (unknown), we targeted systems containing two phosphines and two NHCs. Although mixed NHC/phosphine transition metal complexes[9] have been reported, few examples contain bis-NHCs/bis-phosphines,[9h–k] and none involve iron. Assembling two distinct sets of bidentate ligands to form a heteroleptic complex is precedented for tuning a metal's reactivity and/or stability;[9j,10] however, this approach has not been employed to improve N_2 activation.

Our design strategy employed a methylene-linked bis-NHC ligand, because it is a neutral bidentate ligand with similar steric profile and bite-angles to depe (Fig. 1C).[2d,11] We hypothesized that

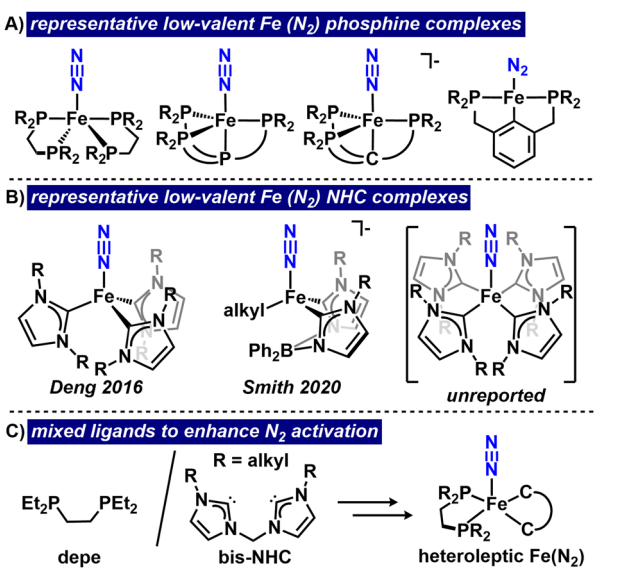

Fig. 1 (A) Fe phosphines demonstrated to activate N_2.[2c,d,g,6a] (B) Fe N_2 NHC complexes and the lack of a reported Fe N_2 tetracarbene.[7b,c] (C) Analogy between depe and bis-NHC ligand and the prospect of a heteroleptic complex.

Department of Chemistry, University of Michigan, 930 North University Avenue, Ann Arbor, MI 48109, USA. E-mail: nszym@umich.edu

† Electronic supplementary information (ESI) available. CCDC 2368195, 2390974 and 2394085. For ESI and crystallographic data in CIF or other electronic format see DOI: https://doi.org/10.1039/d4cc05463f

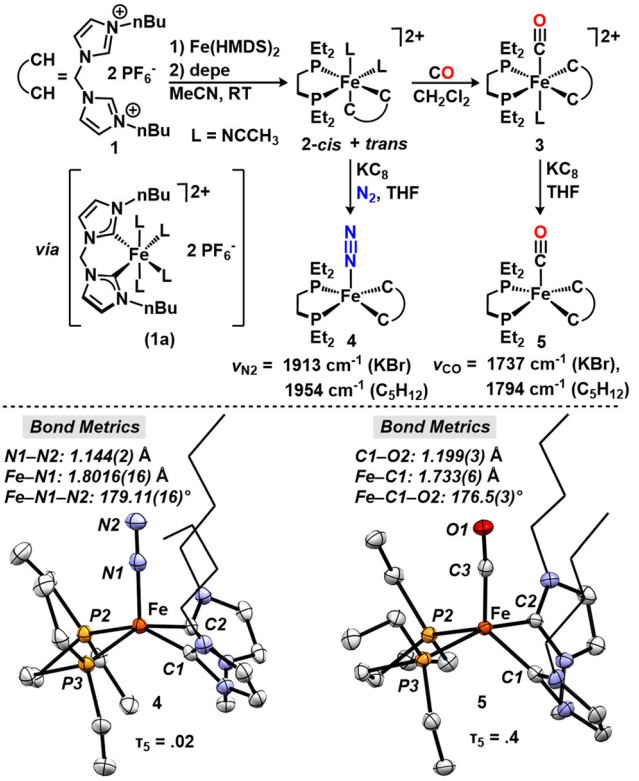

Scheme 1 Synthesis of heteroleptic complexes **2–5**. Molecular structure of **4** determined by single crystal XRD. Thermal ellipsoids shown at 50% probability with hydrogen atoms omitted and non-interacting alkyl chains are in wireframe for clarity.

a heteroleptic iron complex of both a bis-phosphine and a bis-NHC ligand would be structurally analogous to the established bis-(bis-phosphine) $Fe^0(depe)_2$ system, but better able to promote substrate activation with a more electron-rich iron centre.

We developed a general one-pot metalation/ligand substitution procedure (Scheme 1), to access a mixed NHC/phosphine system. Introduction of 1 equiv. **1** (bis-*N*-butyl-imidazolium salt) to a suspension of $Fe(N(SiMe_3)_2)_2$ in CH_3CN afforded a clear red solution after 2 h at room temperature. Solvent removal by vacuum followed by washing with THF yielded a deep red solid. This red intermediate exhibited two aromatic ^{1}H NMR singlets at 7.46 and 7.32 ppm without further downfield resonances, consistent with a symmetrically bound bis-NHC tetrakis-MeCN complex (**1a**) analogous to a previous report.[12] To a CH_3CN solution of **1a** was added 1.0 equiv. depe as a CH_3CN solution, which caused a colour change to deep orange. Concentration of this product under vacuum yielded a viscous solution, from which residual depe was removed *via* pentane extraction. Solvent removal yielded a bright orange diamagnetic complex **2** as a mixture of isomers in 95% yield.

ESI-mass spectrometry of **2** provided a *m/z* of 567.2671, consistent with $[Fe(HCOO)(^{butyl}CC)(depe)]^+$ (*m/z* = 567.2674),¶ which features a heteroleptic composition of the primary coordination sphere. The ^{1}H NMR spectrum in CH_2Cl_2 exhibited a set of four strong aromatic singlets (7.53, 7.38, 7.28, & 7.04 ppm) and a set of two weaker singlets (7.58 and 7.24 ppm) that integrate in a net ratio of ∼ 6 : 1. The ^{31}P NMR spectrum exhibited a pair of doublets (75.87 and 62.93 ppm, J_{PP} = 15Hz) and a smaller singlet (62.56 ppm) that integrate to the same ratio (Fig. S2 and S3, ESI†). This pattern is consistent with a mixture of the *cis*-heteroleptic isomer (**2**-*cis*), where both phosphorus and NHC donors are inequivalent, and the *trans* heteroleptic isomer (**2**-*trans*), where they are equivalent. Following addition of MeCN-d_3 to **2**, we observed a loss of coordinated MeCN ^{1}H NMR resonances (2.45 and 2.33 ppm) and growth of free MeCN (1.94 ppm). This behavior indicates facile exchange of MeCN ligands and may implicate a ligand exchange pathway for isomerization of **2**. The structure of **2**-*cis* was further confirmed by single crystal x-ray diffraction (SC-XRD) studies from crystals grown in CH_2Cl_2.

Although **2** was isolated as a mixture of *cis* and *trans* isomers, we found that addition of a neutral π-acid, such as CO, afforded a *single* geometric isomer. Charging a solution of **2** in CH_2Cl_2 with 30 psig CO caused the colour to slowly fade over 6 h. Evaporation of the solvent afforded a pale-yellow species (**3**). Its ^{31}P NMR spectrum featured a singlet at 64.6 ppm, while the ^{1}H NMR spectrum exhibited aromatic resonances at 7.57 and 7.17 ppm that integrate 4:3 with a singlet at 2.48 ppm. This result is consistent with a *trans* geometry (C_s symmetry) containing a single acetonitrile ligand. ESI mass spectrometry of **3** provided a *m/z* of 295.6467, consistent with $[Fe(CO)(MeCN)(^{butyl}CC)(depe)]^{2+}$ (*m/z* = 295.6451). IR spectroscopy of **3** revealed a single ν_{CO} stretch at 1947 cm^{-1}. These data support assignment of **3** as a heteroleptic complex containing a single carbonyl ligand *trans* to a coordinated CH_3CN. We attribute formation of the *trans* isomer of **3** to the strong *trans* donor properties of CO, which favours *trans* ligands that are weaker donors (MeCN), rather than stronger donors (NHC or phosphine), as would be necessitated by the *cis* isomer.

Following the synthesis of **2** and **3**, we pursued an Fe^0 species. Reduction of **2** with excess KC_8 followed by pentane extraction/removal afforded a deep red diamagnetic solid (**4**). This species exhibits a sharp ^{31}P NMR singlet at 90.05 ppm, and two aromatic ^{1}H singlets at 6.44 and 6.35 ppm. Subjecting **3** to analogous reduction conditions and workup yielded a diamagnetic orange solid (**5**). NMR spectra of **5** similarly exhibit a broad ^{31}P NMR singlet at 95.85 ppm and two ^{1}H singlets at 6.45 and 6.32 ppm. The breadth of these NMR resonances of **4** and **5** vary with temperature (−75 °C to 45 °C), indicating fluxionality in solution.

Both **4** and **5** exhibited more activated π-acceptor ligands than their bis-depe Fe^0 analogues: **4** displayed a strong ν_{N2} stretch at 1913 cm^{-1} (ν_{N_2} = 1955 cm^{-1} for $FeN_2(depe)_2$) and **5** exhibited a strong ν_{CO} stretch at 1737 cm^{-1} (ν_{CO} = 1800 cm^{-1} for $FeCO(depe)_2$). The ligand environment imposed on iron was assessed using cyclic voltammetry experiments. Compounds **4** and **5** exhibited reversible events at −2.48 V and −2.06 V (THF, *vs.* $Fe(Cp_2)/Fe(Cp)_2^+$), respectively, which we assign as Fe(0/1) redox couples. Relative to the bis-depe analogues, **4** and **5** are significantly more reducing (480 mV and 520 mV more cathodic, respectively[2a]), further supporting strongly reduced Fe centers.

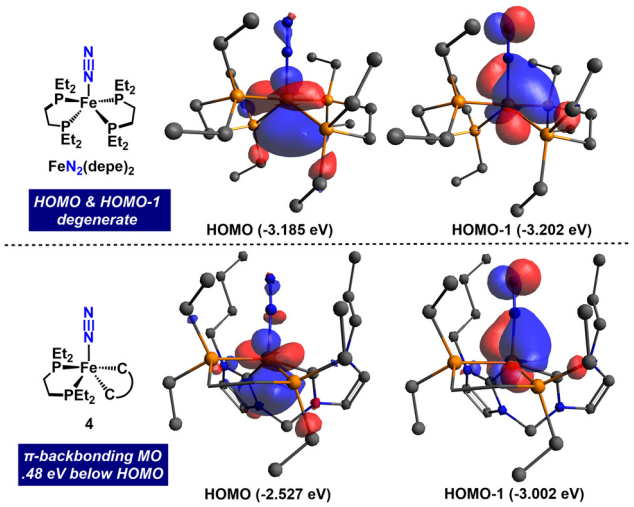

Fig. 2 Frontier orbitals from DFT performed at TPSS def2-TZVP level of theory with SMD solvation model on optimized structure (isosurface values = 0.05).

SC-XRD studies on **4** and **5** reveal structural differences from the analogous $Fe(depe)_2$ complexes. **5** exhibits an intermediate 5-coordinate (τ = 0.4) geometry and **4** has a square pyramidal (τ = 0.02) geometry, which contrast with the reported TBP geometry of $FeN_2(depe)_2$ and $FeCO(depe)_2$ (τ = 0.9 for both).[7b,13] While the N–N bond distance of **4** is not statistically different from that of $FeN_2(depe)_2$, (1.144(2) Å *vs.* 1.139(13) Å), the C–O bond of **5** is longer than that of $FeCO(depe)_2$ (1.199(3) Å *vs.* 1.179(8) Å), consistent with its more activated IR stretch. Both the Fe–N_2 bond of **4** and the Fe–CO bond of **5** are longer than their $Fe(depe)_2$ analogues (1.8016(16) Å *vs.* 1.748(8) Å for FeN_2; 1.733(6) Å *vs.* 1.179(8) Å for FeCO), which reflects less multiple bond character between iron and the bound diatoms, despite greater π-backdonation (Scheme 1).

Geometry optimization of both **4** and **5** using density functional theory (DFT) converged to intermediate structures (τ = 0.4). IR spectra and Fe(0/1) redox potentials for both $FeN_2(depe)_2$ and **4** calculated from these DFT optimization studies corroborate solution-phase experimental results (Table S4, ESI†), supporting the intermediate geometry as the solution-phase structure of **4**. This optimized structure also reveals an elongated N–N bond in **4** with respect to $FeN_2(depe)_2$ (1.142 Å *vs.* 1.139 Å), indicating increased activation of the N_2 ligand. Molecular orbital (MO) calculations for **4** and $FeN_2(depe)_2$ illustrate energetic differences between the frontier orbitals (Fig. 2). The HOMO of **4** is localized on the Fe centre, is σ-antibonding with respect to N_2 coordination, and higher in energy than that of $FeN_2(depe)_2$, which validates elongated Fe–N_2 and Fe–CO bonds found in crystal structures of **4** and **5**.

The HOMO-1 of **4** is the primary orbital involved in π-backdonation into the N_2 π* orbital; however it is −0.475 eV lower than the HOMO. Despite the HOMO-1 being higher in energy in **4** than in $FeN_2(depe)_2$, this orbital sits far below the metal-centred HOMO. This electronic structure renders the complex more basic at Fe, and less likely to protonate at N_2 than for $FeN_2(depe)_2$. We attribute the higher orbital energies of **4** to the greater donor strength of the NHC ligands, while the distortion of its geometric and electronic structure is due to the inherent asymmetry of the heteroleptic ligand environment.

To augment the DFT studies that predict high Fe-basicity of **4**, we studied its reactivity with Brønsted acids. Treating **4** with $[NH_2Ph_2][OTf]$ in THF afforded a rapid color change from red to yellow. This product exhibits a triplet ^{1}H NMR resonance spectrum at −16.7 ppm ($^2J_{HP}$ = 60 Hz), a doublet ^{31}P NMR resonance at 81.9 ppm ($^2J_{HP}$ = 59 Hz), and an IR absorbance at 2072 cm^{-1}. These data are consistent with prior reports of $[FeH(N_2)]^+$ complexes,[2a,k] as protonation of $FeN_2(depe)_2$ with 1 equiv. $[NH_2Ph_2][OTf]$ afforded *trans*-$[Fe(H)N_2(depe)_2]^+$, characterized by a ^{1}H NMR quintet at −18.20 ppm, a ^{31}P doublet at 81.14 ppm ($^2J_{HP}$ = 50 Hz), and an IR feature at 2090 cm^{-1} (ν_{N2}). Therefore we assign this product as *trans*-$[FeH(N_2)(depe)(^{butyl}CC)][OTf]$ ([**6**][OTf]) (Fig. 3). Treatment of **4** with a weaker acid, ^{t}BuOH, affords **6** quantitatively by NMR spectroscopy, but subjecting $FeN_2(depe)_2$ to the same conditions yields <15% protonation. This divergence in reactivity demonstrates the higher basicity of the Fe center predicted by DFT in **4** compared to $FeN_2(depe)_2$.

To minimize Fe-centered reactivity, we targeted a more sterically encumbered electrophile, trimethylsilyl triflate ($SiMe_3OTf$), for N_2 functionalization, analogous to reported silylation of $FeN_2(depe)_2$.[14] Addition of 1 eq of $SiMe_3OTf$ to an Et_2O solution of **4** at −78 °C afforded a deep green precipitate (**7**) in 75% yield (Fig. 3). This species exhibits a ^{31}P NMR singlet at 85.3 ppm, and two aromatic ^{1}H singlets at 7.68 and 7.16 ppm, which is consistent with a Fe^{II} heteroleptic complex. These aromatic features integrated net 4 : 9 with respect to a ^{1}H singlet at 0.19 ppm, consistent with incorporation of one $SiMe_3$ group. A single ^{19}F NMR resonance at −78.9 ppm is consistent with a free triflate anion in the product, indicating a cationic iron complex. ^{29}Si NMR spectroscopy revealed a singlet at -5.4 ppm, and ATR-IR characterization of **7** exhibited a strong absorbance at 1693 cm^{-1}; both of which are consistent with a silyldiazenide ($^-$NNSiMe_3) substituent. These spectra are similar to those of the reported $[Fe(N_2SiMe_3)(depe)_2]^+$ (N_2SiMe_3 unit = ^{1}H NMR: 0.20 ppm, ^{29}Si NMR: 6.4 ppm, IR: 1732 cm^{-1}).[14] In contrast to the reaction of $FeN_2(depe)_2$ with $SiMe_3OTf$, which was reported to be reversible, **7** formed cleanly and irreversibly, supporting the increased basicity of the N_2 moiety of **4**. Compared to other reported iron silyldiazenido complexes, of which most are neutral,[1b,15] the IR absorbance suggests that **7** is among the most activated, only surpassed by an anionic example[1b] from the Holland group, despite assignment of **7**

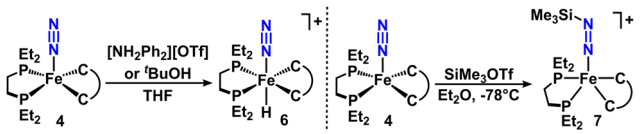

Fig. 3 Synthesis of **6** and **7** from **4**.

as cationic. While the heteroleptic iron system and $Fe(depe)_2$ demonstrate similar aptitude for N_2 silylation, each heteroleptic intermediate (the N_2 (**4**) and silylhydrazide (**7**) complexes) exhibit substantially more activated N–N bonds at each step.

In conclusion, we have reported the synthesis and characterization of a new class of heteroleptic Fe^0 complexes jointly supported by a bis-phosphine and a methylene-linked bis-NHC ligand. The dinitrogen and carbonyl complexes, **4** and **5**, are highly reduced, as exemplified by their highly activated ν_{N2}/ν_{CO} stretches and cathodic redox potentials. SC-XRD and DFT studies reveal that both **4** and **5** adopt an intermediate 5 coordinate geometry (τ = 0.4). Silylation of **4** yields a highly activated silydiazenido complex **7**, demonstrating the system's potential for N_2 functionalization. This mixed-ligand Fe^0 system exhibits properties uncharacteristic of reported Fe^0 phosphine or NHC complexes, and the modular access to heteroleptic Fe^0N_2 compounds presented herein invites further work to tune the primary sphere donors and induce new reactivity at iron.

C. A. performed the experiments. N.K.S managed the project. Both C. A. and N. K. S. designed and analysed experiments and wrote the manuscript.

This work was supported by the NIH (R35GM136360). We thank Fengrui Qu for SCXRD collection of **2**-*cis*, **4**, and **5** and the Buss Lab for assistance with inert atmosphere IR spectroscopy.

Data availability

The data supporting this article have been included as part of the ESI.† Crystallographic data for 2-*cis*, **4**, and **5** have been deposited at the CCDC under and can be obtained from **https://www.ccdc.cam.ac.uk/structures**.

Conflicts of interest

There are no conflicts to declare.

Notes and references

‡ For N_2, we use the term "activation" to refer to a lower N–N bond order, assessed structurally, or by IR spectroscopy (ν_{N2}).[16]
§ A notable exception is the ligand DMeOPrPE.[5c]
¶ Formate ($HCOO^-$) is present in the ESI-MS eluent solution.

1 (*a*) J. S. Anderson, J. Rittle and J. C. Peters, *Nature*, 2013, **501**, 84; (*b*) S. F. McWilliams, D. L. J. Broere, C. J. V. Halliday, S. M. Bhutto, B. Q. Mercado and P. L. Holland, *Nature*, 2020, **584**, 221; (*c*) M. M. Rodriguez, E. Bill, W. W. Brennessel and P. L. Holland, *Science*, 2011, **334**, 780–783; (*d*) S. Kuriyama, K. Arashiba, K. Nakajima, Y. Matsuo, H. Tanaka, K. Ishii, K. Yoshizawa and Y. Nishibayashi, *Nat. Commun.*, 2016, **7**, 12181; (*e*) S. M. Rummelt, H. Zhong, I. Korobkov and P. J. Chirik, *J. Am. Chem. Soc.*, 2018, **140**, 11589.
2 (*a*) P. J. Hill, L. R. Doyle, A. D. Crawford, W. K. Myers and A. E. Ashley, *J. Am. Chem. Soc.*, 2016, **138**, 13521; (*b*) M. M. Deegan and J. C. Peters, *J. Am. Chem. Soc.*, 2017, **139**, 2561; (*c*) S. Kuriyama, T. Kato, H. Tanaka, A. Konomi, K. Yoshizawa and Y. Nishibayashi, *Bull. Chem. Soc. Jpn.*, 2022, **95**, 683; (*d*) M. Hirano, M. Akita, T. Morikita, H. Kubo, A. Fukuoka and S. Komiya, *Dalton Trans.*, 1997, 3453; (*e*) M. V. Baker and L. D. Field, *Organometallics*, 1986, **5**, 821; (*f*) H. H. Karsch, *Chem. Ber.*, 1977, **110**, 2213; (*g*) S. E. Creutz and J. C. Peters, *J. Am. Chem. Soc.*, 2014, **136**, 1105; (*h*) T. T. Adamson, S. P. Kelley and W. H. Bernskoetter, *Organometallics*, 2020, **39**, 3562; (*i*) D. J. Schild and J. C. Peters, *ACS Catal.*, 2019, **9**, 4286; (*j*) T. A. Betley and J. C. Peters, *J. Am. Chem. Soc.*, 2004, **126**, 6252; (*k*) L. D. Field, N. Hazari and H. L. Li, *Inorg. Chem.*, 2015, **54**, 4768; (*l*) G. J. Leigh and M. Jimenez-Tenorio, *J. Am. Chem. Soc.*, 1991, **113**, 5862; (*m*) A. Hills, D. L. Hughes, M. Jimenez-Tenorio, G. J. Leigh and A. T. Rowley, *Dalton Trans.*, 1993, 3041.
3 J. B. Geri, J. P. Shanahan and N. K. Szymczak, *J. Am. Chem. Soc.*, 2017, **139**, 5952.
4 (*a*) H. Corona, M. Pérez-Jiménez, F. de la Cruz-Martínez, I. Fernández and J. Campos, *Angew. Chem., Int. Ed.*, 2022, **61**, e202207581; (*b*) A. D. Piascik, R. Li, H. J. Wilkinson, J. C. Green and A. E. Ashley, *J. Am. Chem. Soc.*, 2018, **140**, 10691.
5 (*a*) R. A. Cable, M. Green, R. E. Mackenzie, P. L. Timms and T. W. Turney, *J. Chem. Soc. Chem. Commun.*, 1976, **7**, 270; (*b*) A. M. Tondreau, B. L. Scott and J. M. Boncella, *Organometallics*, 2016, **35**, 1643; (*c*) J. D. Gilbertson, N. K. Szymczak and D. R. Tyler, *J. Am. Chem. Soc.*, 2005, **127**, 10184.
6 (*a*) R. Gilbert-Wilson, L. D. Field, S. B. Colbran and M. M. Bhadbhade, *Inorg. Chem.*, 2013, **52**(6), 3043–3053; (*b*) L. D. Field, H. L. Li, S. J. Dalgarno and R. D. McIntosh, *Eur. J. Inorg. Chem.*, 2019, 2006–2011; (*c*) F. F. van de Watering, W. Stroek, J. Ivar van der Vlugt, B. de Bruin, W. I. Dzik and J. N. H. Reek, *Eur. J. Inorg. Chem.*, 2018, 1254–1265; (*d*) D. E. Prokopchuk, E. S. Wiedner, E. D. Walter and C. V. Popescu, *et al.*, *J. Am. Chem. Soc.*, 2017, **139**(27), 9291–9301; (*e*) A. Cavaillé, B. Joyeux, N. Saffon-Merceron, N. Nebra, M. Fustier-Boutignon and N. Mézailles, *Chem. Commun.*, 2018, **54**(84), 11953.
7 (*a*) Y. Fan, J. Cheng, Y. Gao, M. Shi and L. Deng, *Chem. Sin.*, 2018, **76**, 445; (*b*) Z. Ouyang, J. Cheng, L. Li, X. Bao and L. Deng, *Chem. – Eur. J.*, 2016, **22**, 14162; (*c*) S. A. Lutz, A. K. Hickey, Y. Gao, C.-H. Chen and J. M. Smith, *J. Am. Chem. Soc.*, 2020, **142**, 15527.
8 C. R. Groom, M. P. Lightfoot and S. C. Ward, *Acta Crystallogr.*, 2016, **B72**, 171.
9 (*a*) A. Ahmida, F. M. Elmagbari, H. Egold, U. Flörke and G. Henkel, *Polyhedron*, 2020, **181**, 114472; (*b*) A. Ahmida, F. M. Elmagbari, H. Egold and G. Henkel, *Polyhedron*, 2021, **198**, 115083; (*c*) P. Ai, A. A. Danopoulos and P. Braunstein, *Dalton Trans.*, 2016, **45**, 4771; (*d*) B. R. Galan, E. S. Wiedner, M. L. Helm, J. C. Linehan and A. M. Appel, *Organometallics*, 2014, **33**, 2287; (*e*) P. Nagele, U. Herrlich, F. Rominger and P. Hofmann, *Organometallics*, 2013, **32**, 181; (*f*) E. Mosaferi, L. Pan, T. Wang, Y. Sun, C. Pranckevicius and D. W. Stephan, *Dalton Trans.*, 2016, **45**(4), 1354; (*g*) N. Stylianides, N. Tsoreas and A. A. Daopoulos, *J. Organomet. Chem.*, 2005, **690**, 5948; (*h*) X. Liu and W. Chen, *Dalton Trans.*, 2011, **41**(2), 599; (*i*) O. Bárta, P. Pinter, I. Císařová, T. Strassner and P. Štěpnička, *Eur. J. Inorg. Chem.*, 2020, 575–580; (*j*) A. L. Ostericher, K. M. Waldie and C. P. Kubiak, *ACS Catal.*, 2018, **8**(10), 9596; (*k*) M. V. Baker, S. K. Brayshaw, B. W. Skelton, A. H. White and C. C. Williams, *J. Organomet. Chem.*, 2005, **690**(9), 2312.
10 (*a*) S. Gonell, E. A. Assaf, J. Lloret-Fillol and A. J. M. Miller, *ACS Catal.*, 2021, **11**(24), 15212; (*b*) Y. Liu, K. S. Kjær, L. A. Fredin, P. Chábera and T. Harlang, *et al.*, *Chem. – Eur. J.*, 2015, **21**(9), 3628; (*c*) K. Witas, S. S. Nair, T. Maisuradze, L. Zedler, H. Schmidt and P. Garcia-Porta, *et al.*, *J. Am. Chem. Soc.*, 2024, **146**(29), 19710.
11 S. Meyer, C. M. Orben, S. Demeshko, S. Dechert and F. Meyer, *Organometallics*, 2011, **30**(24), 6692.
12 J. Rieb, A. Raba, S. Haslinger, M. Kaspar, A. Pöthig, M. Cokoja, J.-M. Basset and F. E. Kühn, *Inorg. Chem.*, 2014, **53**, 9598.
13 S. Komiya, M. Akita, A. Yoza, N. Kasuga, A. Fukuoka and Y. Kai, *J. Chem. Soc. Chem. Commun.*, 1993, **9**, 787.
14 A. D. Piascik, P. J. Hill, A. D. Crawford, L. R. Doyle, J. C. Green and A. E. Ashley, *Chem. Commun.*, 2017, **53**, 7657.
15 (*a*) Y. Ohki, K. Munakata, Y. Matsuoka, R. Hara, M. Kachi, K. Uchida, M. Tada, R. E. Cramer, W. M. C. Sameera and T. Takayama, *et al.*, *Nature*, 2022, **607**, 86–90; (*b*) M.-E. Moret and J. C. Peters, *J. Am. Chem. Soc.*, 2011, **133**, 18118; (*c*) Y. Lee, N. P. Mankad and J. C. Peters, *Nat. Chem.*, 2010, **2**, 558; (*d*) J. Rittle and J. C. Peters, *Proc. Natl. Acad. Sci. U. S. A.*, 2013, **110**, 15898.
16 J. L. Crossland and D. R. Tyler, *Coord. Chem. Rev.*, 2010, **254**, 1883.

